Structural Engineering and Mechanics, *Vol. 94*, *No. 5* (*2025*) *325-334*
https://doi.org/10.12989/sem.2025.94.5.325

High-temperature performance of coconut fibre-reinforced coral concrete

Cunpeng Liu[1,2a], Fatimah De'nan*[2], Pengyong Deng[3b], Qian Mo[3c], Dalian Bai[1d] and Li Liang[3e]

[1]*Department of Civil and Surveying Engineering, Guilin University of Technology at Nanning, 530001, Nanning, Guangxi, China*
[2]*School of Civil Engineering, Engineering Campus, Universiti Sains Malaysia, 14300, Nibong Tebal, Pulau Pinang, Malaysia*
[3]*Department of Civil and Architectural Engineering, Guangxi Transport Vocational and Technical College, 530023, Nanning, Guangxi, China*

(*Received June 25, 2024, Revised March 1, 2025, Accepted April 9, 2025*)

Abstract. Coconut fibre is low carbon and environmentally friendly and has a low cost, relatively high strength and toughness, and can be incorporated into concrete to improve the latter's resistance to high-temperature bursting. In this study, an appropriate amount of coconut fibre was added to coral concrete to simultaneously solve the problems of low early strength, large shrinkage and poor resistance to high-temperature bursting of coral concrete and to initially establish the theoretical system of coconut fibre-reinforced coral concrete (CF-CC) to lay a theoretical foundation for solving the intrinsic defects of coral concrete and expanding its engineering applications. The results show that there is no obvious cracking in the specimen above 700°C.At 900°C, many cracks penetrated the specimen. At 20–100°C, the specimen mass loss was very low. At 300°C, the specimen mass loss rate was approximately 9%. Afterwards, the change in mass loss rate with temperature was relatively small. The compressive strength peaked at 100°C, with a maximum increase of nearly 10%, and decreased considerably at 300°C, with a maximum decrease of 16.5%. At 500°C, the average compressive strength decreased by approximately 10%. The compressive strength–temperature curve tended to stabilise. At 20°C, the addition of coconut fibres with densities of 3–4.5 kg/m^3 considerably enhanced the tensile strength, with a maximum increase of approximately 20%. Then, at 100°C, the addition of coconut fibre slightly increased the coral concrete tensile strength, with a maximum increase of 7.5%. Above 100°C, coconut fibre minimally affected the coral concrete tensile strength.

Keywords: coconut fibre; coral concrete; high temperature; mechanical properties; numerical fitting

1. Introduction

Modern coral reefs in China are mainly distributed in the South China Sea Islands and along the northern coast. The islands and reefs in the South China Sea are primarily composed of coral reefs (Cai *et al.* 2021). Although these structures formed relatively recently in history, they serve as precious land resources in the vast ocean. The surrounding fishery and mineral resources are very abundant, and they have critical geographical benefits. These resources are the bases for development in the ocean and for protection of marine rights and interests. Moreover, these materials have become important for deep-sea fishery development, ocean energy development, ocean tourism, transportation, and national defence construction (Su *et al.* 2020). However, island construction has certain problems. Because most islands are far from the mainland, their environment is harsh. In addition, sand, gravel, and freshwater resources are scarce (Li and Cao 2022). Therefore, island construction must consider construction costs and the building material sources. If transported from the mainland, the materials can considerably increase costs. Therefore, reducing construction costs and solving the problems associated with coarse aggregate sources are highly important in island construction. To avoid damaging the local ecological environment, the use of coral aggregates instead of crushed stones, coral sand instead of river sand, and seawater instead of fresh water, as well as preparing coral concrete by mixing with seawater, have great practical importance for civil and military engineering projects on islands.

Coral concrete has the advantages of being easy to obtain and lightweight, but it has several disadvantages, such as a low tensile strength, low compressive strength, and low elastic modulus (Yang *et al.* 2021). To address the common problems of cracking in coral concrete in engineering, relevant researchers (Fergani *et al.* 2018, Wang *et al.* 2018, Jiang *et al.* 2019, Liu *et al.* 2020, Yang *et al.* 2020, Wang *et al.* 2021, Cao *et al.* 2023, Liu *et al.* 2024) have investigated fibre-reinforced coral concrete. By measuring the specific characteristics, including the strength, deformation resistance, and fatigue resistance of the mixture, it can be determined that adding fibres to coral concrete can improve the overall stability of the mixture and enhance its mechanical properties, such as its tensile strength. Although the above methods can effectively

*Corresponding author, Ph.D.
E-mail: cefatimah@usm.my
[a]Ph.D. Student
E-mail: liucunpeng@student.usm.my
[b]B.S.
E-mail: 853111157@qq.com
[c]M.S.
E-mail: 931632781@qq.com
[d]Ph.D.
E-mail: baidl90@163.com
[e]M.S.
E-mail: 236713979@qq.com

ISSN: 1225-4568 (Print), 1598-6217 (Online)

Table 1 Seawater parameters

Ion	Ion concentration of seawater (mg/L)
Na^+	9050
K^+	566.5
Ca^+	380.5
Mg^{2+}	1150
SO_4^{2+}	2235
Cl^-	16118

improve the mechanical properties of coral concrete, artificial fibres, such as polypropylene, carbon, and glass fibres, add considerable challenges in use, such as high energy consumption and high carbon emission levels. Moreover, artificial fibres are expensive and do not yet fulfil the requirements for widespread use. Therefore, a green, environmentally friendly, and cost-effective fibre with good mechanical properties must be found to solve the problems of coral concrete. Coconut fibres processed from coconut shells have high strength and toughness, low cost, low carbon and environmental protection. In addition, coconut fibre can delay the hydration reaction of cement to reduce the hydration heat of fresh concrete (Maojun and Guoping 2024) and form steam channels at high temperatures to improve the concrete's resistance to high-temperature bursting. CF has better tensile performance and toughness than other natural fibres, and it can be used to compensate for the disadvantages of high brittleness and easy cracking ability in cement-based materials (Ali *et al.* 2012, Ahmad *et al.* 2020, 2021).

To adapt to the application of coral concrete in high-temperature environments, such as in airport runways and in nuclear waste treatment, and to evaluate the performance after an engineering fire, the high-temperature performance of coral concrete must be studied. Scholars (Guo 2021, Liu 2021, Zhou *et al.* 2023) have researched the compressive strength, tensile strength, elastic modulus, and constitutive relationship of coral concrete that has been exposed to high temperatures, the degradation effect of high temperature on the coral concrete and GFRP bars at the interface increases with increasing temperature, after exposure to high temperature, the bond strength between GFRP bars and coral concrete gradually decreases, and the peak slip gradually increases, the bond stiffness of the splitting failure specimen increases first and then decreases with increasing temperature, while the bond stiffness of the pull-out failure specimen gradually decreases. As the temperature increases, the tensile strength and elongation at break of CF decrease significantly. When the temperature rises to 400°C, CF has been thermal decomposition and basic carbonization, when the temperature rises above 600°C, CF has been completely thermal decomposition (Hui 2022). However, the research method remains incomplete, and the evaluation method is not unified. In this article, the failure characteristics and corresponding mechanical properties of coconut fibre-reinforced coral concrete (CFCC) treated with high temperatures are studied, and the relationships among the mass loss, compressive strength, splitting tensile strength, coconut fibre content, and heating temperature are explored. This study provides a basis for correctly evaluating the bearing capacities and damage degrees of coral concrete specimens mixed with coconut fibre after fire exposure, and it provides a reference for their application in practical engineering.

Fig. 1 Coral sand

Fig. 2 Coral aggregates

2. Experimental raw materials and testing methods

2.1 Experimental raw materials

The cement used is ordinary Portland cement (P·O42.5 grade) from Bohai. The sand is coral sand obtained by crushing the coral aggregate with a powerful crusher (mesh size of 6 mm), as shown in Fig. 1. The mixing water is seawater, and the mix proportion is shown in Table 1. The coarse aggregate is a well-graded coral aggregate, as shown in Fig. 2, the 1-h water absorption rate is 17.8% and the compressive strength is 2.01 MPa. The appearance of the coconut fibre used is shown in Fig. 3, and the various performance indicators are shown in Table 2. The coconut fibre is soaked in water for 2 h, cleaned to eliminate impurities and soaked in a 2% NaOH solution for 2 h. Finally, the sample is washed, dried and cut into approximately 10-mm pieces for later use.

In the experiment, the CF density is the main variable. Five CF-CC specimens are designed with densities of 0 kg/m^3, 1.5 kg/m^3, 3 kg/m^3, 4.5 kg/m^3, and 6 kg/m^3, these specimens are labelled CF-CC0 CF-CC1, CF-CC2, CF-CC3, and CF-CC4, respectively. The design strength grade

Table 2 Performance indicators of coconut fibre average diameter (um)

	1-h water absorption rate (%)	Elongation at break (%)	Tensile strength (MPa)	Elastic modulus (GPa)
250	16.65	21.2–40.7	128–157	3.86–5.86

Table 3 Mix proportions

Number	Water cement ratio	Cement (kg/m^3)	Coral aggregate (kg/m^3)	Coral sand (kg/m^3)	Water (kg/m^3)	Coconut fibre (kg/m^3)
CF-CC0	0.4	450	716	830	180	0
CF-CC1	0.4	450	716	830	180	1.5
CF-CC2	0.4	450	716	830	180	3
CF-CC3	0.4	450	716	830	180	4.5
CF-CC4	0.4	450	716	830	180	6

Note: The water consumption in the table is the net water consumption.

Fig. 3 Coconut fibre

of the concrete is C30, and the specific mix proportions are shown in Table 3.

2.2 Test methods

Coral concrete specimens are produced in accordance with the standard test methods for the physical and mechanical properties of concrete, with design dimensions of 150 mm×150 mm×150 mm. Coral concrete is mixed using a forced mixer. The relatively large clumps of coconut fibres are torn apart, and then the materials are added in the following order: stones, sand, and coconut fibres. First, the specimens are dry mixed for 1 min, wet mixed with ½ the total amount of water for 1 min, and finally mixed with cement and ½ the total amount of water for 1 min. Coconut fibre is filamentous. To avoid agglomeration in concrete after adding water and to ensure its uniformity, coconut fibre is added before water. Under anhydrous conditions, coarse aggregates can disperse agglomerated coconut fibres. Conversely, coral aggregates are porous and have high water absorption rates. However, during mixing, coral aggregates cannot fully absorb water before wetting for 1 h. Before adding the cement, water is added. Once the coral aggregates reach a certain degree of water absorption before wetting, cement is added. This technique can prevent the coral concrete from undergoing layering and segregation during mixing, and it can improve the working performance of this material.

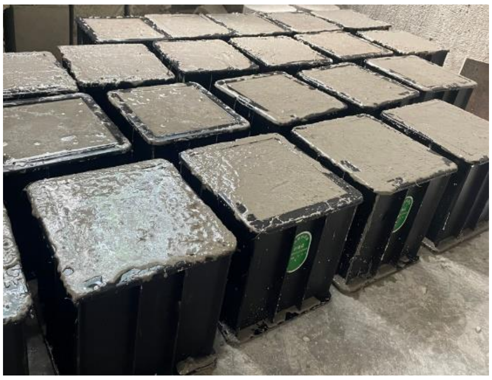

Fig. 4 Vibration-formed specimen

Fig. 5 Curing of specimens

Coconut fibre-reinforced coral concrete is loaded into the mould in two stages. In the first stage, 2/3 of the mould is filled and compacted on a vibration table. Then, the material is loaded above the mould and vibrated on the vibration table for 10–15 s. Finally, the material is compacted with a trowel and repeatedly smoothed, as shown in Fig. 4. After the specimen is cured in air for 24 h, the mould is removed, and the specimen is placed in a curing box, as shown in Fig. 5. After 27 days of curing, the specimen is removed and allowed to stand for 24 h at room temperature before a high-temperature test is conducted. The electric furnace used in the high-temperature test is a box-type resistance furnace with a maximum temperature of 1200°C. The temperature inside the furnace can be automatically controlled. The high-temperature target temperatures specified in this experiment are 20°C, 100°C, 300°C, 500°C, 700°C, and 900°C. The specimens are placed in an electric furnace and heated to the specified target temperature at a rate of 2.5°C/min. After reaching a specific target temperature, the specimens are kept at this temperature for 1 h. The specimens are cooled naturally to room temperature in the furnace.

3. Experimental results and discussion

The appearance, mass loss rate, cubic compressive

Table 4 Appearance of the CF-CC specimens at different temperatures

	20°C	100°C	300°C	500°C	700°C	900°C
CF-CC0	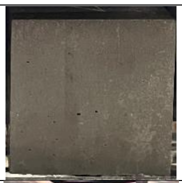					
CF-CC1					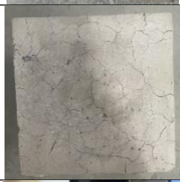	
CF-CC2						
CF-CC3						
CF-CC4					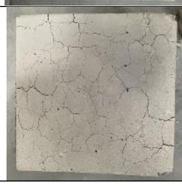	

strength, and splitting tensile strength characteristics of the CF-CC specimens at different temperatures are studied to understand the changes in their mechanical properties from a macroscopic perspective. Then, scanning electron microscopy (SEM) analysis is used to study the changes in the hydration compositions and microstructures and to determine why the mechanical properties of the CF-CC specimens depend on temperature. At 900°C, the compressive strength of the CF-CC specimen is almost completely lost, thus, no mechanical performance tests are conducted at this temperature.

3.1 Appearance characteristics after high-temperature treatment

Table 4 shows the variation in the appearance of each group of CF-CC specimens with temperature. According to a study of the effect of high temperatures on the appearance of CF-CC, the coral concrete matrix develops burst resistance. This burst resistance can help each specimen maintain a high degree of integrity in high-temperature environments. The surface of the CF-CC specimen appears dark grey at 20°C. When the temperature increases to 100°C, the surface of the specimen becomes light brown. None of the numbered specimens exhibit peeling, missing corners, looseness, or bursting, and none of them have visible cracks. When the temperature increases to 300°C, the appearance of the specimen is similar to that at 100°C,

Fig. 6 Morphology after 1 day of standing at 900°C

with a light-yellow surface featuring small pores and microcracks. When the temperature increases to 500°C, all specimens are grey–white, and the surface pores and microcracks are greater than those at 300°C. There are no missing corners, looseness, or explosions in any specimen. When the temperature increases to 700°C, the specimens are still greyish white but have many greyish brown spots. Many microcracks are distributed on the surface of each specimen, and each specimen exhibits slight peeling and missing corners. With increasing CF content, the numbers of pores and microcracks increase slightly. The coral concrete specimen with a CF content of 4.5 kg/m^3 exhibits

Fig. 7 Morphology after 3 days of standing at 900℃

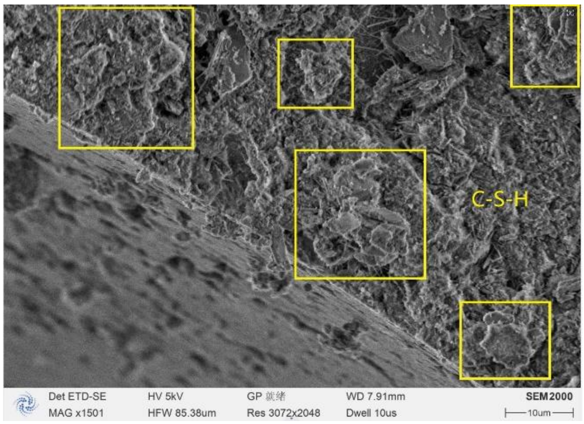

Fig. 8 Coral–mortar interface at 20°C

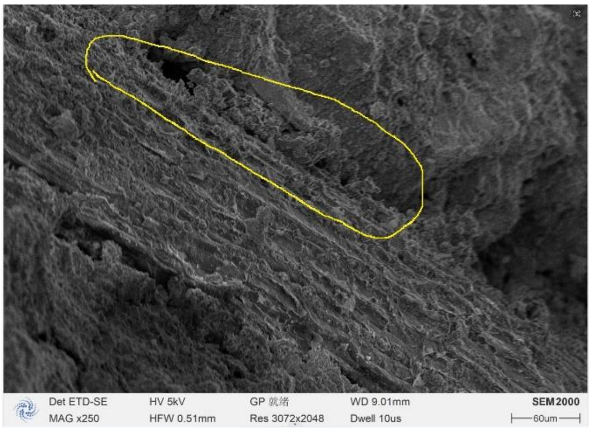

Fig. 9 Fibre–mortar interface at 20°C

slight peeling. When the temperature reaches approximately 900°C, the specimen appears greyish brown, and cracks penetrate the entire outer surface. For example, cracks appear in arid soil. After one day of standing, the concrete continuously peels off the specimen (Fig. 6), after three days, the matrix completely loses its bearing capacity. The mortar and most of the coral aggregates transform into powder-like substances (Fig. 7).

3.2 Microscopic analysis after high-temperature treatment

In this experiment, a relatively flat surface fragment of approximately 2 mm×2 mm is taken from each group of

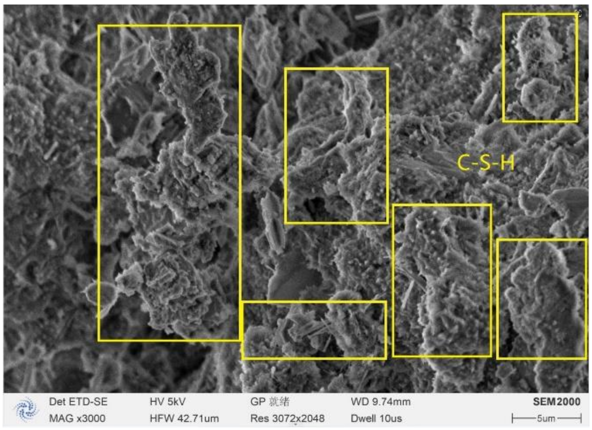

Fig. 10 Coral–mortar interface at 100°C

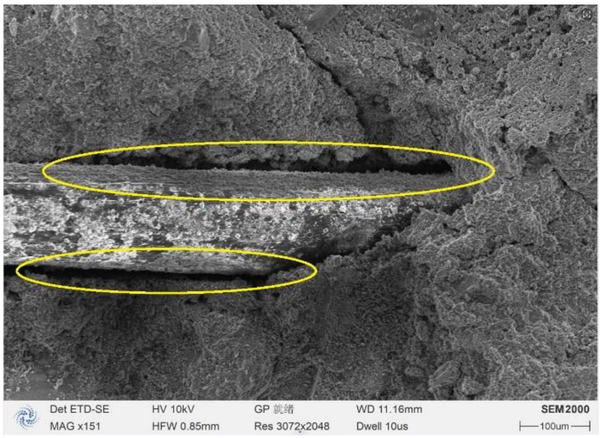

Fig. 11 Fibre–mortar interface at 100°C

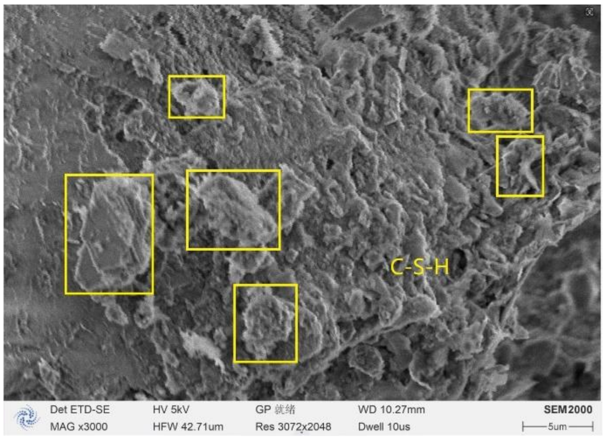

Fig. 12 Coral–mortar interface at 300°C

samples. The microstructure of the sample is observed using SEM. The microstructures of the specimens at different temperatures are shown in Figs. 8-17.

Fig. 8 shows that at 20°C, the overall structure of a specimen is dense, and many layers of regular crystals (C-S-H) are present in the mortar matrix. These crystals overlap uniquely to form a dense specimen. Fig. 9 shows that the surface of the CF is rough, and it can be tightly connected to the mortar matrix through the presence of a mechanical biting force between the two, allowing them to jointly bear the load.

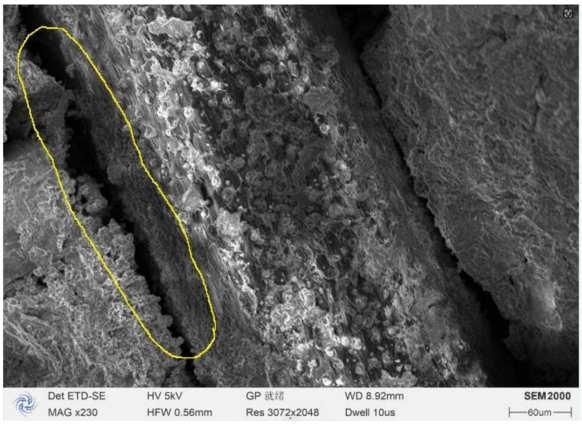

Fig. 13 Fibre–mortar interface at 300°C

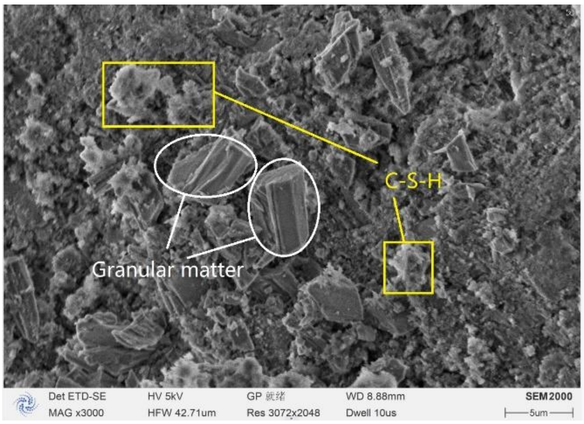

Fig. 14 Coral–mortar interface at 500°C

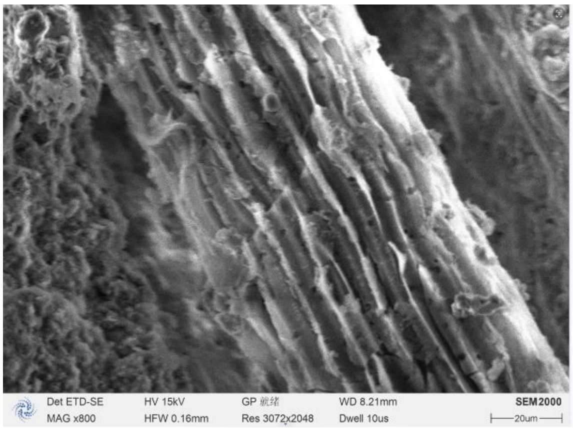

Fig. 15 Fibre–mortar interface at 500°C

When the temperature increases to 100°C, water vapour is formed due to the evaporation of free water. The cement particles that have not matured inside the concrete begin to undergo accelerated hydration under steam curing conditions, resulting in a relatively dense matrix structure, and a large amount of C-S-H is seen in Fig. 10. Moreover, Fig. 11 shows that owing to the increase in temperature, the surface of the CF begins to carbonise and smoothen. In addition, the interface between the fibres and mortar is not tightly bonded to an adequate degree.

When the temperature increases to 300°C, the crystal structure begins to shrink because of the dehydration of C-

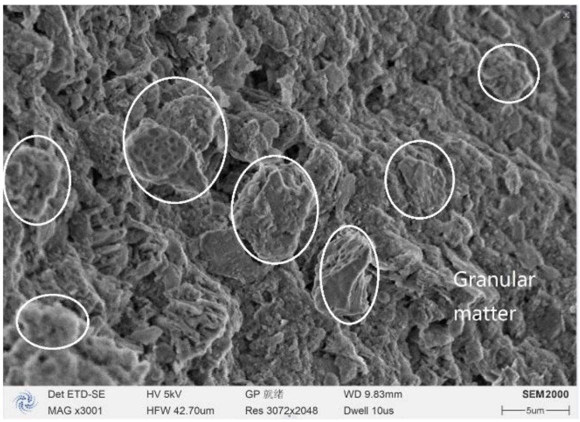

Fig. 16 Mortar at 700°C

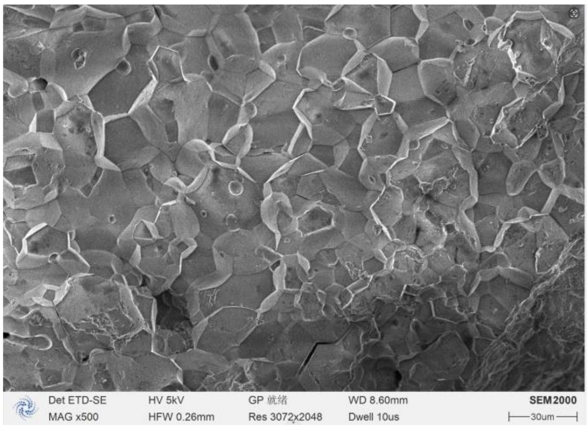

Fig. 17 Cross-sections of coral aggregates at 900°C

S-H, and the overall structure is relatively loose, as shown in Fig. 12. At this point, the CF appearance is not considerably different from that at 100°C. However, the CF volume further decreases, resulting in the formation of additional voids inside the mortar matrix, as shown in Fig. 13.

When the temperature increases to 500°C, the microstructure of the mortar considerably changes, becoming relatively rough. The original C-S-H crystal structure basically disappears, the exposed granular material increases, and the overall density decreases severely, as shown in Fig. 14. Furthermore, Fig. 15 shows that the CF basically carbonises at 500°C. The surface appears fluffy with numerous cracks, and it completely loses its mechanical bearing capacity.

As the temperature increases to 700°C, the microstructure of the mortar does not change substantially, as shown in Fig. 16, differing from the microstructure at 500°C. The matrix is basically granular and has a highly porous structure. At this point, no trace of CF is observed in the mortar matrix. Relevant studies (Wang and Wang 2020) indicate that CFs completely carbonise at 600°C, then, these fibres decompose and oxidise into carbon and nitrogen oxides.

The above information shows that after 900°C is reached and maintained for a period, the specimen has poor integrity. The mortar and most of the coral aggregates transform into powder-like substances, and only a few coral

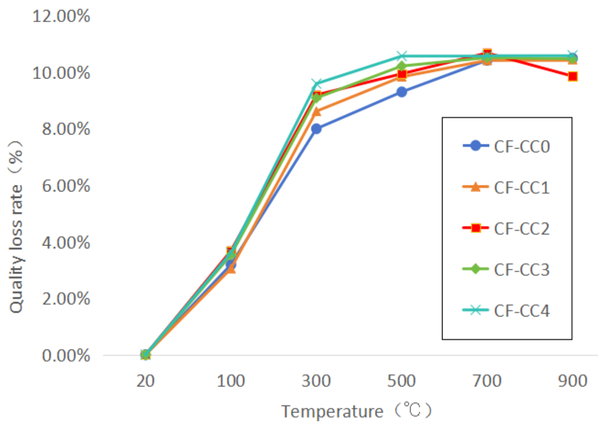

Fig. 18 Quality loss rates of CF-CC specimens at different temperatures

Table 5 Masses of CF-CC specimens at different temperatures (g)

	20°C	100°C	300°C	500°C	700°C	900°C
CF-CC0	7060	6865	6496	6404	6325	6320
CF-CC1	7063	6898	6455	6369	6328	6326
CF-CC2	7077	6817	6427	6374	6322	6380
CF-CC3	7083	6833	6440	6360	6339	6342
CF-CC4	7085	6829	6406	6337	6336	6335

aggregates can remain intact or break into several sections. The cross-section is shown in Fig. 17, and the constituent units are still arranged in an orderly manner. However, many microcracks and small pores are present.

3.3 Quality loss after applying high temperatures

Coral concrete is a heterogeneous composite material whose various components undergo different physical and chemical changes at different high temperatures. These changes are the keys to changing the appearance and quality of concrete that has been exposed to high temperatures. In addition to the abovementioned physical and chemical changes, cracking is a major cause of quality loss in concrete that has been exposed to high temperatures (Khaleel *et al.* 2021). However, during this experiment, the integrity of the specimens is good, and no obvious cracking occurs. Therefore, the physical and chemical changes in the concrete compositions under high-temperature conditions are the main factors causing quality loss. The masses of the CF-CC specimens at different temperatures in this experiment are shown in Table 5.

The relationships between the mass loss rate of each CF-CC specimen and the temperature are shown in Fig. 17.

Fig. 18 shows that as the temperature increases, the overall quality loss rates of the CF-CC specimens increase. The quality loss rates of the specimens increase considerably in the temperature range of 20°C–300°C, but they gradually stabilise as the temperature increases above 500°C.

At 100°C, the mass loss rate of each CF-CC specimen is approximately 3%. Based on the above microstructure analysis, the hydration products in the concrete are chemically stable in this temperature range. The mass loss mainly comes from the internal adsorption of water, the escape of interlayer water, and the mass loss caused by the evaporation of water in the CF.

At 300°C, the mass loss rate of each CF-CC specimen rapidly increases to approximately 9%. The mass loss mainly comes from the evaporation of free water in the concrete. Owing to the large content of free water in the concrete (approximately 95% when freshly mixed and approximately 65%~70% when finally set), the amount of mass lost in each specimen in this temperature range increases rapidly with increasing temperature (Gong *et al.* 2023).

When the temperature increases to 500°C, the mass loss rate of each CF-CC specimen slowly increases to approximately 10%. Owing to the decomposition of the hydration product C-S-H cementitious system, the bound water in the cement slurry is gradually eliminated, but its mass fraction in the concrete is relatively low (Ramanaidu *et al.* 2019). Moreover, the quality loss of the specimen increases with increasing CF content, as CF is basically carbonised at a high temperature of 500°C, resulting in a decrease in fibre quality.

When the temperature is 500–900°C, the mass loss rate of each group of specimens remains basically unchanged compared to that at 500°C.

3.4 Compressive strength after high-temperature treatment

After the CF-CC specimens have experienced different temperatures, their residual compressive strengths are determined through the aforementioned test method, and the

Table 6 Residual compressive strengths of CF-CC specimens at different temperatures (MPa)

	20°C	100°C	300°C	500°C	700°C
CF-CC0	29.3	30.5	25.9	22.8	21.1
CF-CC1	30.3	31.1	24.5	21.4	20.2
CF-CC2	30.5	31.9	25.6	21.7	20.9
CF-CC3	29.1	31.7	24.3	22.1	19.6
CF-CC4	29.6	31.3	25.5	22.4	19.7

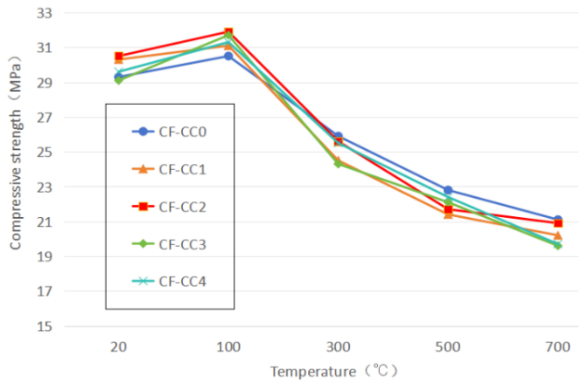

Fig. 19 Residual compressive strengths of the CF-CC specimens at different temperatures

results are shown in Table 6.

Table 6 and Fig. 19 show that the relative residual compressive strengths of different CF-CC specimens are temperature-dependent in accordance with the following trend:

When the temperature increases from 20°C to 100°C, the relative residual compressive strengths of the five different CF-CCs increase, with a maximum increase of 8.9%. According to the above microscopic analysis, mortar accelerates hydration under water vapour to form a dense structure. Owing to the porosity of coral aggregates, the internal pressure caused by water vapour can be alleviated, the premature occurrence of microcracks can be prevented, and the compressive strength of concrete can be improved.

When the temperature increases to 300°C, the relative residual compressive strengths of the five CF-CC samples decrease rapidly by 11.60%, 19.14%, 16.07%, 16.49%, and 13.85%. The strengths of the specimens begin to decrease in this temperature range because water vapour is generated most strongly in the concrete when the temperature is between 100°C and 300°C. Moreover, water vapour cannot escape in time, forming a large pressure inside the concrete, causing the initial defects inside the concrete to rapidly expand and form visible cracks. The increase in strength by steam curing is no longer sufficient to resist the decrease in strength caused by crack propagation, thus, the macroscopic performance of concrete manifests as a decrease in strength (Varghese *et al.* 2021).

When the temperature increases to 500°C, the relative residual compressive strengths of the five CF-CC samples continue to decrease, with decreases of 10.58%, 10.23%, 12.79%, 7.56%, and 10.47%. The strengths of the samples in this temperature range continue to decrease because when the temperature reaches 500°C, the microstructure of the mortar undergoes considerable changes, the structure becomes relatively rough, the original C-S-H crystal structure basically disappears, the amount of exposed granular material increases, and the overall density severely decreases.

When the temperature increases to 700°C, the relative residual compressive strengths of the five CF-CC samples decrease slightly, with an average decrease of 6%. The strength decreases in this temperature range mainly because at this stage, the internal moisture evaporates from the concrete ends, the C-S-H cementitious system begins to decompose and breakdown, and the difference in temperature deformation between the aggregate and cement slurry increases, these changes lead to continuous crack propagation and extension and damage to the concrete structural system, resulting in a decrease in strength (Ramanaidu *et al.* 2019).

From 20°C to 100°C, the experimental compressive strength data fluctuate greatly. A fitting relationship between the residual compressive strength of each numbered CF-CC specimen and temperature is established from 100°C–700°C. The fitting formula is as follows:

CF-CC0: y=15.843*0.998^x+17.980 (100°C≤X≤700°C, R=0.999)

CF-CC1: y=17.994*0.996^x+19.088 (100°C≤X≤700°C, R=0.999)

CF-CC2: y=18.346*0.996^x+19.300 (100°C≤X≤700°C, R=0.995)

CF-CC3: y=19.047*0.996^x+18.613 (100°C≤X≤700°C, R= 0.991)

CF-CC4: y=19.450*0.998^x+15.631 (100°C≤X≤700°C, R= 0.999)

Table 7 Residual tensile strengths of the CF-CC specimens at different temperatures (MPa)

	20°C	100°C	300°C	500°C	700°C
CF-CC0	2.83	2.39	1.22	0.96	0.81
CF-CC1	3.15	2.35	1.35	0.88	0.85
CF-CC2	3.41	2.5	1.28	0.78	0.74
CF-CC3	3.43	2.57	1.34	0.84	0.77
CF-CC4	3.36	2.51	1.39	0.85	0.72

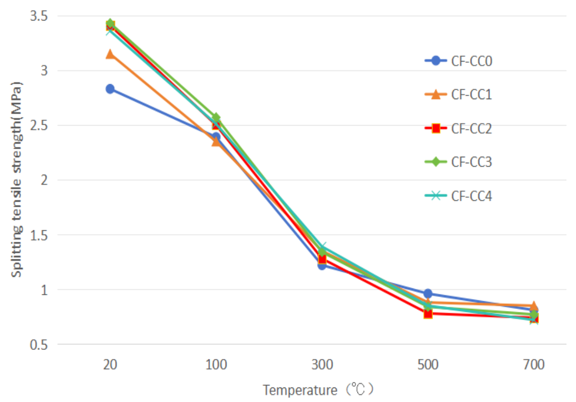

Fig. 20 Residual tensile strengths of the CF-CC specimens at different temperatures

3.5 Tensile strength after high-temperature treatment

After the CF-CC specimens are subjected to different high temperatures, their residual strengths are measured according to the aforementioned test method, and the results are shown in Table 7.

Table 7 and Fig. 20 show that the residual tensile strength of each specimen decreases after a high temperature is reached. The higher the target temperature is, the lower the residual tensile strength. When the temperature increases from 20°C to 300°C, the tensile strength of the coral concrete decreases the most (by 56.89%, 57.14%, 62.46%, 60.93%, and 58.63%). This result arises because the high temperature causes the CF-CC specimens to become brittle, making them highly sensitive to microcracks (Khan *et al.* 2024). At 300–700°C, the residual tensile strengths of the CF-CC specimens vary relatively steadily with temperature. The residual tensile strength is approximately 1 MPa.

The relationship between the tensile strength of coral concrete and the CF content within the range of 20–700°C is shown in Fig. 21. At 20°C, CF considerably enhances the tensile strength of coral concrete. Compared with those of CF-CC0, the tensile strengths of CF-CC1, CF-CC2, CF-CC3, and CF-CC4 increase by 11.31%, 20.49%, 21.20%, and 18.73%, respectively. When the temperature is 100°C, CF slightly increases the tensile strength of coral concrete, with a maximum increase of 7.5%. As the temperature

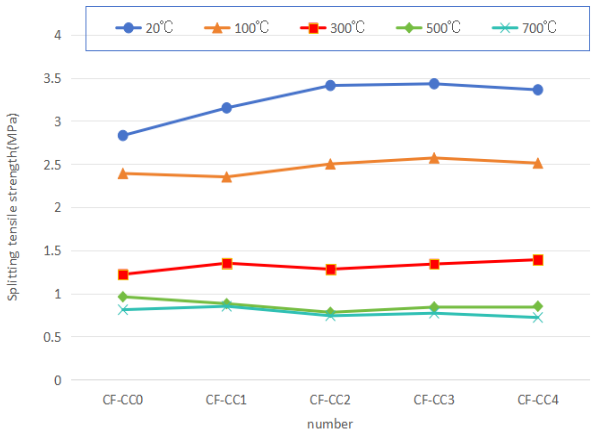

Fig. 21 Relationship between the tensile strength and CF content of coral concrete

continues to increase, the effect of the CF content on the residual tensile strength gradually weakens. This result arises because CF poorly bonds with the mortar matrix at 100–300°C. Moreover, the fibre basically carbonises and loses its bearing capacity at 500°C.

In this article, a fitting relationship is established between the residual tensile strength and temperature of each numbered CF-CC at temperatures ranging from 20°C to 700°C. The fitting formula is as follows:

CF-CC0: y=2.442*0.996^x+0.654 (20°C≤X≤700°C, R=0.988)

CF-CC1: y=2.678*0.995^x+0.731 (20°C≤X≤700°C, R=0.998)

CF-CC2: y=3.123*0.995^x+0.605 (20°C≤X≤700°C, R=0.998)

CF-CC3: y=3.114*0.995^x+0.622 (20°C≤X≤700°C, R= 0.999)

CF-CC4: y=3.054*0.996^x+0.565 (20°C≤X≤700°C, R=0.999)

4. Conclusions

CF-CC is made by mixing coral aggregates and coconut fibres from islands, which considerably reduces the production cost of island construction materials. This technology not only innovates the diversified utilisation model of coconut fibres but also effectively alleviates the dependence of construction projects on inorganic fibres, responding to the requirements for developing green buildings.

The main conclusions are as follows:

(1) Appearance after high-temperature treatment: With increasing temperature, the surfaces of the CF-CC specimens changed from dark grey to light brown, then to light yellow, to greyish white, and finally to greyish brown. The number of surface cracks gradually increased. Above 700°C, no obvious cracking was observed in the specimens. At 900°C, many cracks penetrated the specimens. After several days, the mortar and most of the coral aggregates became powder-like substances.

(2) Microscopic mechanism analysis: At 20°C, the CF and mortar matrix bonded well and could jointly bear stress. At temperatures between 100°C and 300°C, the volume of the CF decreased due to dehydration, thereby decreasing the adhesive bearing capacity of the fibre–mortar interface. The CF underwent carbonisation when the temperature reached or exceeded 500°C, losing its ability to withstand loads. The structures of the mortar matrices were dense at 20°C–100°C, the C-S-H crystal structures shrank at 300°C, and the overall structures were relatively loose. At or above 500°C, the crystal structures basically disappeared, and the overall densities decreased severely.

(3) Mass loss after high-temperature treatment: The mass loss of each specimen was relatively small at 100°C and reached a maximum at 300–500°C. Under the same temperature conditions, as the coconut fibre content increased, the mass loss of a specimen gradually increased. At 500°C–900°C, the quality tended to stabilise.

(4) Compressive strength after high-temperature treatment: The maximum compressive strength was achieved at 100°C, with a maximum increase of nearly 10%. At 300°C, the compressive strength decreased considerably, with a maximum decrease of 16.5%. At 500°C, the average compressive strength decreased by approximately 10%. Afterwards, the curve of compressive strength with temperature tended to stabilise.

(5) Tensile strength after exposure to high temperatures: At 20°C, the addition of CF considerably enhanced the tensile strength of the coral concrete. Compared with those of CF-CC0, the tensile strengths of CF-CC1, CF-CC2, CF-CC3, and CF-CC4 increased by 11.31%, 20.49%, 21.20%, and 18.73%, respectively. At 100°C, CF slightly enhanced the tensile strength of coral concrete, with a maximum increase of 7.5%. As the temperature continued to increase, the effect of CF on the tensile strength of coral concrete became negligible.

Acknowledgments

The authors gratefully acknowledge the financial supports provided By the Middle-aged and Young Teachers' Basic Ability Promotion Project of Guangxi (2024KY1170) and Chongzuo Scientific Research and Technology Development Program Projects (2024ZC017960).

References

Ahmad, J., Aslam, F., Martinez-Garcia, R., Ouni, M.H.E. and Khedher, K.M. (2021), "Performance of sustainable self-compacting fiber reinforced concrete with substitution of marble waste (MW) and coconut fibers (CFs)", *Sci. Rep.*, **11**(1), 23184. https://doi.org/10.1038/s41598-021-01931-x.

Ahmad, W., Farooq, S.H., Usman, M., Khan, M., Ahmad, A., Aslam, F., ... & Sufian, M. (2020), "Effect of coconut fiber length and content on properties of high strength concrete", *Mater.*, **13**(5), 1075. https://doi.org/10.3390/ma13051075.

Ali, M., Liu, A., Sou, H. and Chouw, N. (2012), "Mechanical and dynamic properties of coconut fibre reinforced concrete", *Constr. Build. Mater.*, **30**, 814-825. https://doi.org/10.1016/j.conbuildmat.2011.12.068.

Cai, X., Zhao, Q. and Chen, H. (2021), "Research status of coral concrete", *J. Chin. Ceram. Soc.*, **48**(8), 1753-1764. https://doi.org/10.14062/j.issn.0454-5648.20200951.

Guo, J. (2021), "Study on the static and dynamic mechanical properties of alkaline magnesium sulfate cement coral concrete after high temperature", Master's Thesis, Nanjing University of Aeronautics and Astronautics, Nanjing, China.

Fergani, H., Di Benedetti, M., Oller, C.M., Lynsdale, C. and Guadagnini, M. (2018), "Long-term performance of GFRP bars in concrete elements under sustained load and environmental actions", *Compos. Struct.*, **190**, 20-31. https://doi.org/10.1016/j.compstruct.2018.02.002.

Gong, H., Luo, Y., Wei, X., Peng, J. and Li, X. (2023), "Investigations on dynamic failure behaviors and energy transfer efficiency of heat-treated high-performance concrete under multiaxial constraints", *Constr. Build. Mater.*, **409**, 133930. https://doi.org/10.1016/j.conbuildmat.2023.133930.

Hui, W. (2022), "Research on high temperature properties of coconut fiber magnesium phosphate cement", Master's Thesis, Guangzhou University, Guangzhou.

Jiang, J., Luo, J., Yu, J. and Wang, Z. (2019), "Performance improvement of a fiber-reinforced polymer bar for a reinforced sea sand and seawater concrete beam in the serviceability limit state", *Sensor.*, **19**(3), 654. https://doi.org/10.3390/s19030654.

Khaleel, O.R., Al Wahaibi, M.M.S., Abed, M.J., Dawood, M. and Fayyadh, M.M. (2021), "Performance of carbon fibre concrete subjected to fire", *Mater. Today Proc.*, **42**, 1160-1165. https://doi.org/10.1016/j.matpr.2020.12.530.

Khan, M., Lao, J., Ahmad, M.R. and Dai, J.G. (2024), "Influence of high temperatures on the mechanical and microstructural properties of hybrid steel-basalt fibers based ultra-high-performance concrete (UHPC)", *Constr. Build. Mater.*, **411**, 134387. https://doi.org/10.1016/j.conbuildmat.2023.134387.

Li, X. and Cao, Q. (2022), "Research progress on the mechanical properties of FRP reinforced seawater coral aggregate concrete materials and components", *J. Compos. Mater.*, **39**(3), 926-941. https://doi.org/10.13801/j.cnki.fhclxb.20210902.004.

Liu, B., Li, Y., Wang, Y., Ming, Y., Zhang, X. and Qian, K. (2024), "Uniaxial compression performance of multi-scale hybrid fiber reinforced coral concrete", *J. Ceram.*, **52**(5), 1543-1553. https://doi.org/10.14062/j.issn.0454-5648.20230560.

Liu, B., Zhou, J., Wen, X., Hu, X. and Deng, Z. (2020), "Mechanical properties and constitutive model of carbon fiber reinforced coral concrete under uniaxial compression", *Constr. Build. Mater.*, **263**, 120649. https://doi.org/10.1016/j.conbuildmat.2020.120649.

Ramanaidu, G.D., Jogarao, K. and Ramlal, S. (2019), "A reciprocal research on compressive strength of conventional concrete and carbon fibre concrete exposed to high temperature", *Int. J. Innov. Technol. Explor. Eng.*, **8**(12), 5767-5772. https://doi.org/10.35940/ijitee.k1883.1081219.

Su, C., Ma, H., Yu, H., Yue, C., Zhang, Y., Mei, Q., Sha, H. and Liu, T. (2020), "The influence of different coral aggregates on the mechanical properties of coral concrete", *J. Ceram.*, **48**(11), 1771-1780. https://doi.org/10.14062/j.issn.0454-5648.20200027.

Varghese, A., Anand, N., Andrushia, D. and Arulraj, P. (2021), "Investigation on the performance of fiber reinforced concrete subjected to standard fire exposure", *World J. Eng.*, **18**(3), 442-451. https://doi.org/10.1108/wje-04-2020-0138.

Wang, A., Lyu, B., Zhang, Z., Liu, K., Xu, H. and Sun, D. (2018), "The development of coral concretes and their upgrading technologies: a critical review", *Constr. Build. Mater.*, **187**, 1004-1019. https://doi.org/10.1016/j.conbuildmat.2018.07.202.

Wang, L., Yi, J., Zhang, J., Chen, W. and Fu, F. (2021), "Short-term flexural stiffness prediction of CFRP bars reinforced coral concrete beams", *Mater.*, **14**(2), 467. https://doi.org/10.3390/ma14020467.

Wang, Z. and Wang, T. (2020), "Fire resistance test and analysis of carbon fiber reinforced concrete", *China Saf. Prod. Sci. Technol.*, **16**(11), 77-81.

Yang, S., Yu, M., Dong, K. and Yang, Y. (2020), "Properties of alkali-resistant glass fiber reinforced coral aggregate concrete", *Mater.*, **13**(16), 3450. https://doi.org/10.3390/ma13163450.

Yang, X., Wen, K. and Deng, Z. (2021), "Research on deformation performance and bending rigidity of coral concrete beams reinforced with CFRP", *J. Guangxi Univ. (Nat. Sci. Ed.)*, **46**(1), 19-28. https://doi.org/10.13624/j.cnki.issn.1001-7445.2021.0019.

Zhou, C., Wang, J., Wang, X. and Chen, Z. (2023), "Experimental study on bond behavior of GFRP bar and seawater coral aggregate concrete after exposure to high temperatures", *Acta Mater. Compos. Sin.*, **40**(4), 2224-2239. https://doi.org/10.13801/j.cnki.fhclxb.20220623.001.

CC